An Ultra-Low Output Impedance Power Amplifier for Tx Array in 7-Tesla Magnetic Resonance Imaging

Ashraf Abuelhaija, Klaus Solbach

Abstract—In Ultra high-field MRI scanners (3T and higher), parallel RF transmission techniques using multiple RF chains with multiple transmit elements are a promising approach to overcome the high-field MRI challenges in terms of inhomogeneity in the RF magnetic field and SAR. However, mutual coupling between the transmit array elements disturbs the desirable independent control of the RF waveforms for each element. This contribution demonstrates a 18 dB improvement of decoupling (isolation) performance due to the very low output impedance of our 1 kW power amplifier.

Keywords—EM coupling, Inter-element isolation, Magnetic resonance imaging (MRI), Parallel Transmit.

I. INTRODUCTION

ULTRA -high magnetic field (3T and higher) MRI scanners are promising over lower field MRI scanners in terms of higher SNR and better resolution in MR images. Nevertheless, ultra-high magnetic field systems still face challenges in terms of B_1 inhomogeneity and SAR. In addition to its benefit of speeding up the imaging process, multi-channel parallel RF transmission has been developed to address these challenges by enabling RF shimming. An optimal RF shimming (individual optimization of RF pulse waveform, amplitude and phase for each RF source) of the transmit B_1-field inside the sample requires decoupling of array coils. However, current variation in array coils occurs not only due to mutual coupling but also due to the load change, leading to mismatch between the RF coil and the feed cable. Several decoupling methods have been developed to suppress induced currents in coils and improve the inter-coil isolation of a transmit array. In [1], the vertical loop decoupling method isolates a two-element coil array by generating magnetic flux equal in amount but oppositely oriented to the one generated by the passive element due to mutual coupling. In [2], we presented a high power amplifier with unconventional cartesian feedback loop, which aims at suppressing the coil current variation due to load variation. It can be considered as a promising method to address the issue of inter-coil coupling as well. Current source power amplifiers (PAs) have been shown to be the best option in case isolation between array coils has the priority over the amount of power delivered [3]. An ultra-low output impedance RF power amplifier for 3T MRI systems has been shown to simultaneously deliver maximum

A. Abuelhaija and K. Solbach are with the Department of Electrical Engineering and Information Technology, Institute of High Frequency Technology, Duisburg-Essen University, Oststrae 99, 47057 Duisburg, Germany e-mail: (ashraf.abuelhaija@uni-due.de and klaus.solbach@uni-duisburg-essen.de).
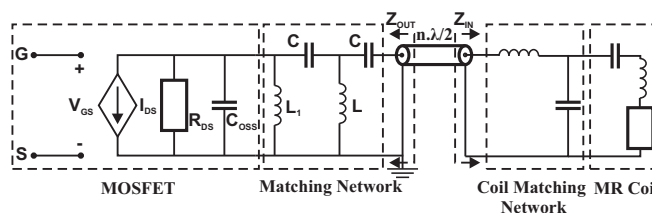
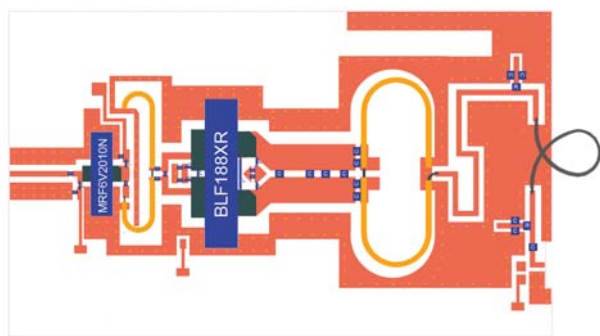Fig. 1: Ultra-low output impedance PA feeding a matched MR coil, after [4].

power to the load and improve the inter-coil isolation of a transmit array [4]. In this paper, load dependence of our high power amplifier (HPA) [5] is studied with an experimental evaluation of its isolation performance for a MR coil combined with our HPA.

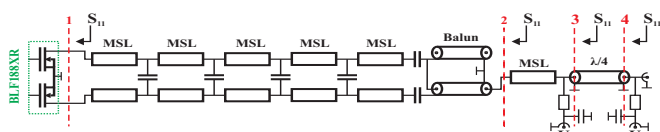## II. COIL DECOUPLING BY PA

The ultra-low output impedance RF power amplifier has been developed by benefiting from the preamplifier decoupling approach for receive coil arrays where the matching networks for receive coils behave like parallel resonant circuits. They transform the low input impedance of the preamplifiers to a high impedance at the coil, thus limiting the current flowing in each coil and the inter-coil isolation is improved. In order to be able to apply the same decoupling approach for parallel transmit, the power amplifier must present low impedance to the coil. The tuning strategy that has been followed in [4] is illustrated in Fig. 1. The power MOSFET can be modeled as voltage-controlled current source once it operates in the saturation region of its DC-characteristic. The current source (I_{DS}) characterized by a high drain-source resistance (R_{DS}). The inductor (L_1) resonates the drain-source capacitance (C_{OSS}) so the MOSFET's output presents a high impedance. The T-section matching network (C-L-C) is tuned for large signal power match while it transforms the drain-source resistance (R_{DS}) to a very low output impedance (Z_{OUT}). The coil matching network up-transforms the low coil impedance to Z_{IN} = 50 Ω. With the low output impedance seen into the PA, the coil sees a parallel resonant circuit which minimizes induced current due to inter-coil coupling.

III. HPA DESIGN

Our HPA has been designed to work at Larmor frequency for 7T (298 MHz) to deliver up to 1 kW RF power to the matched load. It consists of two amplification stages: the

World Academy of Science, Engineering and Technology
International Journal of Electrical and Computer Engineering
Vol:9, No:8, 2015

(a)

(b)

Fig. 2: (a) Simulation setup in ADS software for 2-stage 1 kW power amplifier for 7T MRI, (b) An output matching network in the last amplification stage.

Fig. 3: The DC output characteristic for single transistor of BLF188XR .

Fig. 4: Reflection coefficients for reference planes 1-4.

MRF6V2010 in a driver stage and the BLF188XR LDMOS push-pull transistor pair in a balanced final stage as illustrated in Fig. 2. The transistors have been biased to operate the HPA in class AB. The gate voltage of the final stage was fixed to 2V to bias the drain current to 4.88 A at 50 V drain voltage. This bias setting allows the BLF188XR transistor to operate in the saturation region of its DC-characteristic. To calculate the DC drain-drain resistance (R_{DD}), a DC output characteristic plot of the transistor is required. For a single transistor of the BLF188XR pair, R_{DS} can be obtained from Fig. 3 by calculating the inverse of the slope of the I-V curve in the saturation region. The result that we obtain is 442.5 Ω. For both transistors of the BLF188XR pair, this result should be doubled. However, this result is valid only at DC, whereas the AC measurement result appears different . Based on our AC simulation, and when the power amplifier is powered, the output impedance of the transistor by measuring directly between both drain terminals at reference plane 1 in Fig. 2(b) is 0.261-j*4.759 Ω and the corresponding reflection coefficient is 0.99∠-169°, seen in Fig. 4. In [4], a shunt inductor (L_1) is proposed at the output of the transistor to resonate the drain-source capacitance (C_{OSS}), thus the output of the transistor presents a high impedance. For our case this concept fails, since by adding a shunt inductor (2.55 nH) to resonate the capacitive part, we only get a pure resistance value of 87 Ω as shown in Fig. 4. Because of this relatively low impedance, an alternative matching concept than that proposed in [4] has been employed to fulfill the ultra-low output impedance amplifier requirement.

In Fig. 2, a multistage matching network is seen which increases the band of frequencies of matching for the balanced transistors in combination with a symmetrical balun to transform the coil impedance (nominally 50 Ω) to the optimum value for large signal power transfer. From load pull simulation, and under the same bias condition mentioned previously, the optimum resistance value has been found
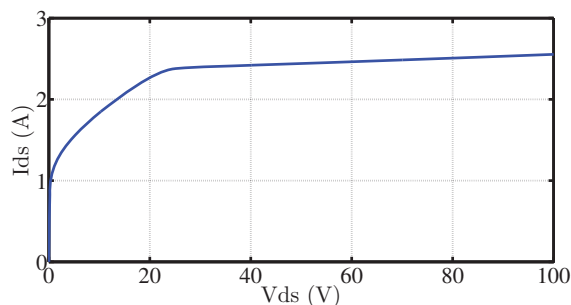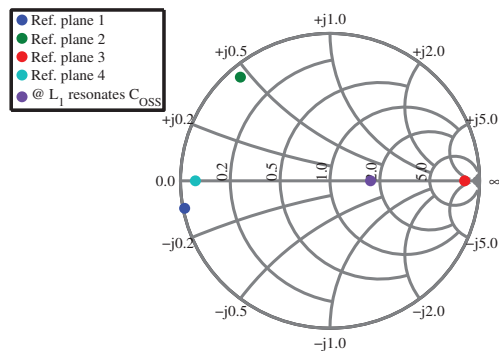
around 2 Ω. This matching network transforms the AC drain-drain impedance (Z_{dd}) seen at reference plane 1 to an impedance which has a reflection coefficient of 0.924∠130° at reference plane 2. This reflects the influence of the matching network on Z_{dd} which behaves like a low impedance transmission line with ca. $\lambda/12$ electrical length. A 50 Ω MSL has been added after the balun to provide an electrical delay so the output impedance seen at reference plane 3 is high with corresponding reflection coefficient of 0.90∠0°, seen in Fig. 4. A quarter-wave transmission line is responsible to turn the high output impedance into a low output impedance with corresponding reflection coefficient of 0.90∠180°at reference plane 4. This matching and electrical delay concept ensure simultaneously a maximum power transfer and very low output impedance for inter-coil isolation.

IV. Load Dependence Characterization

In conventional MR systems, circulators are used in the transmit chains between the power amplifiers and the transmit coil elements in order to isolate the power amplifier from any reflected wave which might appear due to load mismatch or mutual coupling. To evaluate the decoupling performance of our amplifier, a comparison between two transmit chain setups is performed. Fig. 5(a) shows a setup with circulator while Fig. 5(b) shows a direct connection setup. Both setups employ a variable load impedance to emulate either mismatch or mutual coupling phenomena. For an extreme case of coupling that might occur in parallel excitation systems where the coupling factor between array coils is very high, the reflection coefficient (Γ) of the variable load has been selected to vary between -2 and +2. In the following study, and for large signal

World Academy of Science, Engineering and Technology
International Journal of Electrical and Computer Engineering
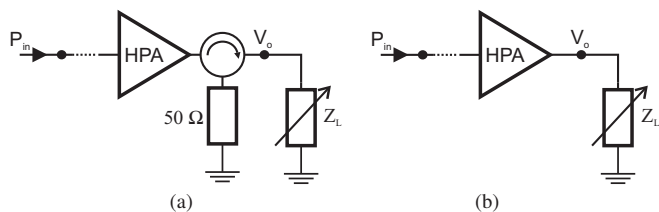Vol:9, No:8, 2015

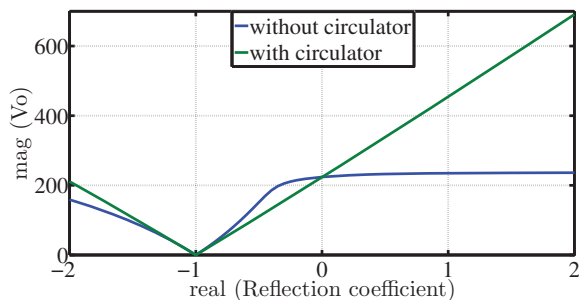Fig. 5: (a) Conventional transmit chain setup, (b) Connection w/o circulator.

Fig. 6: Magnitude of output voltage for both setups under the sweep of the real reflection coefficient between -2 and 2.

operation, our amplifier is driven to deliver 500 W peak power to 50 Ω load corresponding to a peak voltage V_o of around 225 V. In order to obtain an isolation between array coils by suppression of induced current, the HPA should behave like a voltage source (low output impedance), meaning that the output voltage value should be maintained for all load impedance values. Fig. 6 shows the output voltages for both setups by sweeping the real reflection coefficient.
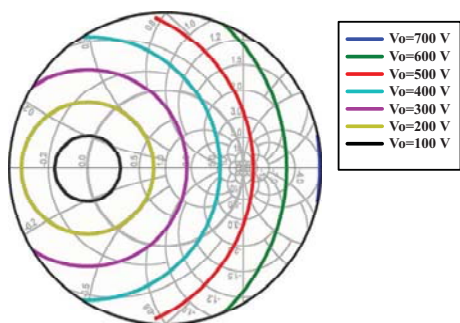

Fig. 7: Contours of magnitude of output voltages for HPA with circulator. Smith chart defined by $-2 < | \Gamma | < 2$ and $-180° < \angle\Gamma < 180°$.
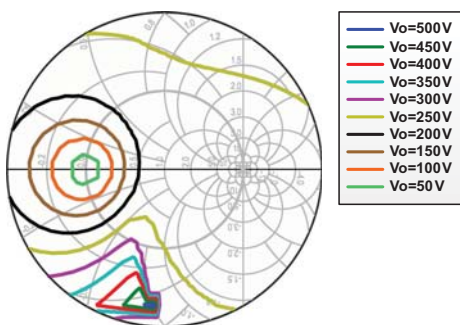

Fig. 8: Contours of magnitude of output voltages for HPA w/o circulator. Smith chart defined by $-2 < | \Gamma | < 2$ and $-180° < \angle\Gamma < 180°$.

The first observation from these two curves is that both curves naturally intersect in two points : when $\Gamma = 0$ and

(matched load), and when $\Gamma = -1$ (short circuit load). When $-1 < \Gamma < 0$, the power amplifier in direct connection setup tries to push up the output voltage levels to reach the matched load level. For $\Gamma > 0$, the increase of the output voltage over the matched load level is negligible. For $-2 < \Gamma < -1$, the direct connection setup has no advantages over the conventional setup. In general cases of variable load, the reflection coefficient can represent a complex value instead of real value. Therefore, the output voltages are better represented as iso-contours cover the smith chart area. Fig. 7 shows a uniform distribution of the output voltage contours for conventional setup, whereas Fig. 8 shows the distribution due to direct connection with less variation for high impedances.

Fig. 9 compares a test result obtained by driving the PA to deliver 670 W peak power to 50 Ω load under the sweep of the real reflection coefficient between -1 and 1. A good agreement between simulated and measured results is noticeable.
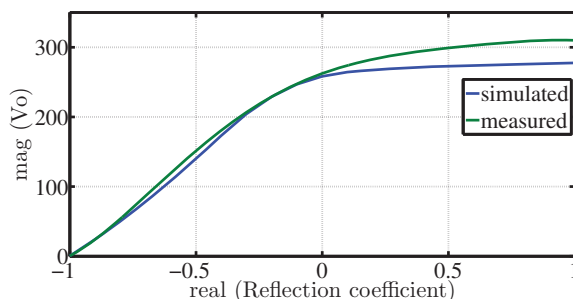

Fig. 9: Simulated and measured output voltage at 670 W peak power for direct connection setup under the sweep of the real reflection coefficient between -1 and 1.

V. COIL DECOUPLING PERFORMANCE BY HPA

In our measurement, a meander coil with high-dielectric substrates [6] has been employed as shown in Fig. 10. A pair of geometrically decoupled pick-up loops placed over the meander coil measures the isolation provided by different types of load (open, short, 50 Ω) and in addition by loading with the HPA output (the HPA powered but inactive). From Fig. 11, we can see the coupling due to the HPA termination to be close to the behaviour of the short circuit termination. We can observe that the highest coupling occurs by open circuit (O.C.) termination as this permits the highest current to flow in the coil. The lowest coupling is seen by short circuit (S.C.) termination because this produces infinite impedance in series with the coil impedance, prohibiting any current to flow. In Table 1, coupling results are normalized to the case of the matched termination to produce a measure of isolation of coils from neighbouring coils. As a result, we find our HPA allows an improvement of 18.7 dB over the conventional 50 Ω termination.

The performance of PA decoupling has also been investigated by EM-simulation of two coupled meander coils as seen in Fig. 12 , where the first element (on the left side) is fed by 1 W accepted power while the second element (on the right side) is either matched terminated as in Fig. 12(a) or terminated by the HPA output reflection coefficient as in Fig. 12(b). Numerical simulation was performed using

World Academy of Science, Engineering and Technology
International Journal of Electrical and Computer Engineering
Vol:9, No:8, 2015

TABLE I
ISOLATION MEASURED FOR DIFFERENT TYPES OF TERMINATION.

Termination	Isolation (dB)
S.C.	32.8
PA	18.7
O.C.	-5.23
50 Ω	0

a FDTD tool (CST Microwave Studio) by simulating two parallel aligned meander coils with 100 mm gap distance and 200 mm below a homogeneous phantom ($\varepsilon_r = 45.3$, $\sigma = 0.8$ S/m). Due to high coupling between the two meander coil elements ($S_{21} = -9.61$ dB in the case of 50 Ω termination), strong induced current flows in the coupled element, producing strong magnetic field, as seen in Fig. 12(a). Contrary, Fig. 12(b) shows a much smaller field around the coupled coil element when it is terminated by the HPA.

VI. CONCLUSION

Our ultra-low output impedance PA has proved its capability to isolate the transmit coil elements and to deliver maximum power to the load simultaneously. A modified output matching network for balanced transistors by taking in to account the electrical delay on the PCB has been presented. A considerable improvement on output voltage variation has been realized by the direct connection setup over the conventional connection setup. Measurement and EM simulation results show a significant improvement in suppressing coupling effects between two coupled meander coils. The length of (lossy) cables should be limited in order to avoid reduction of the high PA output reflection coefficient which would lead to a reduction of the achieved isolation.
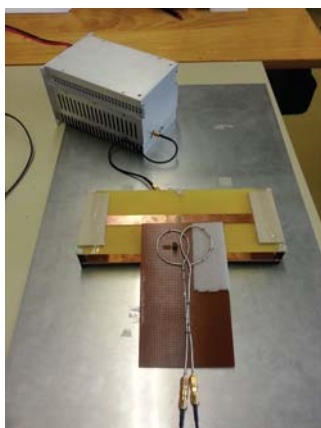
Fig. 10: Coupling measurement setup using two decoupled pick-up loops placed over a meander coil terminated by the HPA.
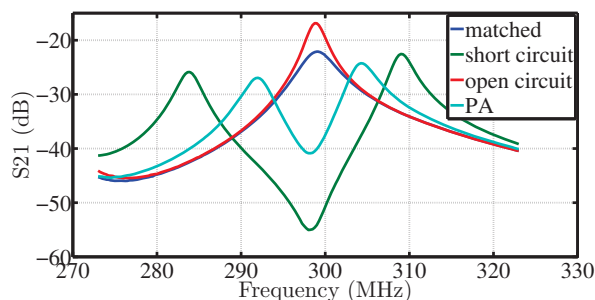

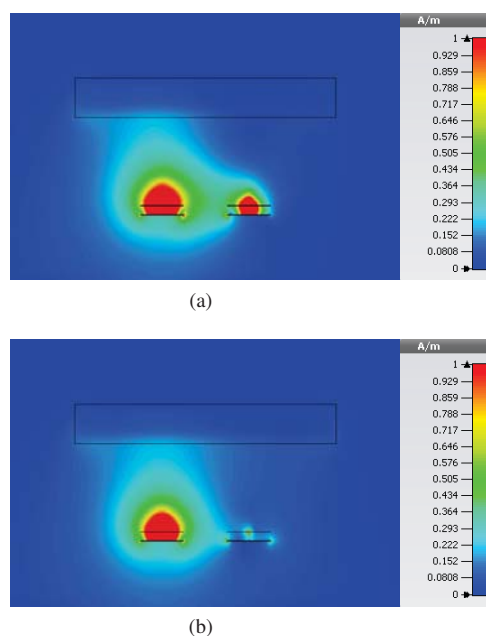Fig. 11: Measured coupling through coil with different coil terminations.

(a)

(b)

Fig. 12: $| H |$ in mid-transversal section for coupled meander coils as seen in FDTD simulator. (a) The second element is matched terminated, (b) The second element is terminated by the HPA output impedance.

REFERENCES

[1] Y. Soutome, Y. Otake, and Y. Bito, "Vertical loop decoupling method for gapped phased-array coils," in *Proc. Intl. Soc. Mag. Reson. Med*, vol. 19, 2011, p. 1859.

[2] A. Abuelhaija, K. Solbach, and A. Buck, "Power amplifier for magnetic resonance imaging using unconventional cartesian feedback loop," accepted to be published in GeMiC, 2015.

[3] N. Hollingsworth, K. Moody, J.-F. Nielsen, D. Noll, M. P. McDougall, and S. M. Wright, "Tuning ultra-low output impedance amplifiers for optimal power and decoupling in parallel transmit MRI," in *Biomedical Imaging (ISBI), 2013 IEEE 10th International Symposium on*. IEEE, 2013, pp. 946–949.

[4] X. Chu, Y. Liu, J. Sabate, and Y. Zhu, "Ultra-low output impedance RF power amplifier array," in *Proc. Intl. Soc. Mag. Reson. Med*, vol. 15, 2007, p. 172.

[5] K. Solbach, A. Abuelhaija, and S. Shooshtary, "Near-magnet power amplifier with built-in coil current sensing," in 22nd *Proc. Intl. Soc. MRM, p. 1287*, 2014.

[6] A. Abuelhaija, K. Solbach, and S. Orzada, "Comprehensive study on coupled meandered microstrip line rf coil elements for 7-Tesla magnetic resonance imaging," accepted to be published in EUCAP, 2015.